Synthesis and Characterization of Surfactant-Stabilized Pt/C Nanocatalysts for Fuel Cell Applications

J. Prabhuram,[†] X. Wang,[†] C. L. Hui,[‡] and I-Ming Hsing*[,†,‡]

Department of Chemical Engineering, and Environmental Engineering Graduate Program, Hong Kong University of Science and Technology, Clear Water Bay, Kowloon, Hong Kong

Received: June 24, 2003; In Final Form: August 7, 2003

Platinum nanocatalysts supported on Vulcan XC-72 carbon have been synthesized through the reduction of chloroplatinic acid with formic acid, using surfactant tetraoctylammonium bromide (TOAB) as the stabilizer in the solvent tetrahydrofuran (THF). These nanocatalysts are synthesized by changing the molar ratio of TOAB to chloroplatinic acid, i.e., N/Pt ratio of 0.76, 0.38, and 0.19. A control catalyst that does not contain TOAB is also synthesized by this method for comparison purposes. Comparison of the morphological properties of these catalysts by transmission electron microscopy (TEM) reveals that the N/Pt ratio of 0.76 catalyst has well-separated smaller particles (2.2 nm) than the other lower molar ratio and control catalysts. X-ray diffraction (XRD) analysis indicates the presence of platinum in the fcc phase and the average size of the particles calculated from the XRD peak widths agreed well with the TEM results. X-ray photoelectron spectroscopic (XPS) measurement of the 0.76 ratio catalyst reveals that a higher amount of Pt exists in its metallic state (73.64% of Pt(O) and 26.36% Pt(II)) and the data are on par with that of the E-TEK catalyst. Stabilization effect of the TOAB on the surface of platinum particles has been discussed with respect to the different N/Pt molar ratios. The XPS technique has been exploited to prove the presence of coverage of TOAB and its subsequent removal from the surface of the Pt particles, which is considered to be the crucial step prior to the electrochemical measurements. Electrochemical measurements have demonstrated that the surface area of the 0.76 ratio catalyst is higher than that of the lower molar ratios (0.38 and 0.19).

Introduction

Nanoparticles are unique materials and have a broad application in the homogeneous and in the heterogeneous catalysis.[1] The uniqueness of these nanoparticles is mainly because of their large surface area and specific functions which are different from those of either bulk metal particles. It is well-known that the higher surface area, which relates to the increase of reacting sites, could be achieved when the size of particles decreases.[2] In recent years, substantial efforts have been made to synthesize Pt nanoparticles (2−10 nm) on the different carbon supports and characterize them by means of X-ray absorption,[3] nuclear magnetic resonance spectroscopy,[4] and infrared spectroscopies.[5] This size range of Pt nanoparticles is of particular interest not only in view of their use in commercial applications but also because of the discernible changes in particle electronic and structural properties.[3−5] Though there have been contradictory conclusions regarding the influence of size and surface structure of these nanoparticles on the electrocatalytic activity, these remain the subject of interest.[1g,6,7] These distinct properties of Pt nanoparticles have enabled them to be employed as catalytic materials for fuel cells to meet the key requirements such as higher electrocatalytic activity and to achieve the reduction in the amount of precious noble metal catalysts. Nevertheless, the synthesis of such nanoscale particles with good dispersion over the carbon black support as an electro-catalytic material remains to be a challenging and tedious work. Therefore, the necessity arises to adopt a special type of the synthetic strategies to obtain the well-dispersed nanocatalytic particles on the supporting materials.

In this context, it is essential to mention some of the recent studies, which have been able to achieve well-dispersed nanoparticles over the supporting materials such as Vulcan XC-72, carbon nanotubes, carbon nanospheres, and carbon fiber nanocomposites. Interestingly, Lee et al.[1h] prepared well-defined Pt and its alloy naoparticles of size 1.7 nm on the Vulcan XC-72 carbon in nonaqueous phase, and this work assumed significance because of not using any protective agents to stabilize the particles. Recently, Che et al. [8] were able to fill the very narrow size Pt−Ru alloy particles (1.59 nm) in carbon nanotube membranes by way of immersing a C/alumina membrane in the solution containing corresponding metal salts and the resulting mass was subjected to reduction in H_2 atm at 580 °C. A similar type of preparative approach has also been followed by Rajesh et al.[9] for loading Pt and its alloy nanoparticles (1−10 nm) on the carbon nanotube for methanol oxidation reaction. Liu et al.[10] were able to produce Pt nanoparticles on the carbon nanotubes by an electroless plating method that was facilitated by two-step sensitization and activation processes. The other fascinating preparative approaches that could achieve the highly dispersed platinum and its alloy nanoparticles on carbon nanotubes are the solid-state reaction of the metal salts with carbon nanotubes at 873 K under a flow of H_2,[11] and simply by mixing the carbon nanotubes with molecular cluster compounds such as $[Ru_5C(CO)_{14}Pt-(COD)]$ and $[PPN][Ru_6C(CO)_{16}SnC_{l3}]$ in organic solvents and allowed it to evaporate in air at room temperature.[12] Serp et al.[13] have adopted a low-temperature

* Author to whom correspondence should be addressed. Fax: (852) 2358-0054. E-mail: kehsing@ust.hk.
[†] Department of Chemical Engineering.
[‡] Environmental Engineering Graduate Program.

10.1021/jp0357929 CCC: $25.00
Published on Web 09/13/2003

chemical vapor deposition method to deposit platinum nanoparticles of mean size of 5 nm on the carbon nanospheres by using the precursor [$PtMe_2(\eta^4\text{-}C_8H_{12})$] in a fluidized bed reactor. The new synthetic strategies reported by Steigerwalt et al.[14] for the preparation of Pt−Ru/carbon nanocomposites (4.8−8.6 nm) have attracted much interest because of its high performance as direct methanol fuel cell anode catalysts. They employed a multistep deposition procedure to achieve the desired loading of Pt−Ru over the carbon composite by using the single-source molecular precursor of Pt and Ru metal ($\eta\text{-}C_2H_4$) (Cl) Pt ($\mu\text{-}Cl)_2Ru(Cl)$ in organic phase.

Though these different preparative procedures could yield varying sizes of nanocatalytic materials, it is strongly believed that the controlled and desired size of the catalytic particles can be achieved by stabilizing the particles either by using surfactants or solvents.[1a−c,15] The probable stabilization mechanism of the surfactant molecule that covered the particles can be explained on the basis of an electrostatic effect, where the hydrophobic part is assembled on the particle surface and the charged hydrophilic or lipophilic group is pointed toward the other end which causes electrostatic repulsion between particles.[1a−c] Once the catalytic particles are stabilized, the quantitative removal of the surfactants which is necessary for the electrochemical measurements could be achieved by annealing the catalysts at high temperature in a flow of N_2 or H_2 gas, followed by the treatment with ethanol.[1a−c] So far, to the best of our knowledge, very few studies have been published in the direction of synthesizing surfactant-stabilized electrocatalytic materials on the high-surface-area carbon support.[1e,15b−c] Among them, it is of particular interest to point out the study of Bonnemann et al.,[15b−c] who synthesized the surfactant-stabilized bimetallic $Pt_{0.5}Ru_{0.5}N(Oct)_4Cl$ colloids (2.4 nm) supported on Vulcan carbon XC-72 in THF solvent for H_2/CO and CO oxidation. Recently, in our group, Wang and Hsing[1e] have synthesized Pt and Pt−Ru nanocatalysts (2−3 nm) on Vulcan XC-72 by the simple alcohol reduction method with the usage of the surfactant dodecyldimethyl (3-sulfo-propyl) ammonium hydroxide (SB12). The electrochemical activity of these catalysts was found to be identical to that of the commercial E-TEK catalyst.

In the present investigation, for the first time, we report the synthesis of 20 wt % Pt nanoparticle on the Vulcan XC-72, stabilized by means of the surfactant tetraoctylammonium bromide (TOAB) and using formic acid as a reducing agent in the organic solvent THF. The TOAB is carefully chosen because of its advantages of long-chained tetraoctylammonium ions, which favors a smaller size of the particles and it could be easily removed from the particle surface after the stabilization process.[1a−c] The nanocatalyst is synthesized by changing the molar ratio between TOAB to chloroplatinic acid, i.e., N/Pt ratio of 0.76, 0.38, and 0.19, respectively. The well-dispersed smaller size (2.2 nm) catalytic particles, which is considered to be the state of the art fuel cell catalyst,[15a] can be obtained when the N/Pt ratio is maintained at 0.76. The electrochemical activity of this 0.76 ratio catalyst is found to be superior to that of the other lower molar ratio and control catalysts.

Experimental Section

Materials. All the chemicals used were of analytical grade. Hexachloroplatinic acid and surfactant tetraoctylammonium bromide were purchased from Aldrich. Tetrahydrofuran (THF), methanol, and ethanol (all from Fischer Scientific Company) were used as received. Formic acid and sulfuric acid were obtained from Merck. Vulcan XC-72 carbon and 20 wt % Pt/Vulcan carbon were procured from E-TEK. Nafion 5% solution was obtained from Dupont and was used as received.

Characterization Methods. Transmission electron microscope (TEM) images were obtained by using a high-resolution JEOL 2010 TEM system operated with LaB6 filament at 200 KV. The samples were dispersed in ethanol under sonication and dropped on the carbon-coated grid and then imaged. X-ray diffraction (XRD) patterns of the nanocatalyst loaded on carbon were obtained with Philips Powder Diffraction System (model PW 1830) using a Cu Kα source operated at 40 keV at a scan rate of 0.025° s^{-1}.

The X-ray photoelectron spectroscopic (XPS) measurements of the nanocatalysts were carried out with a Physical Electronics PHI 5600 multi-technique system using Al monochromatic X-ray at a power of 350 W. The survey and regional spectra were obtained by passing energy of 187.85 and 23.5 eV, respectively.

The filtrate that was obtained after filtering the heterogeneous Pt/C mixture was analyzed by an inductively coupled plasma atomic emission spectrometer (ICPAES) (Perkin-Elmer, Optima 3000XL) after calibration with a standard solution containing a known amount of metal content.

Synthesis of Pt Colloids in THF. Three catalysts with N/Pt molar ratios of 0.76, 0.38, and 0.19 and one control catalyst (without TOAB) were synthesized. For synthesizing Pt/C with N/Pt ratios of 0.76, 0.38, and 0.19, the corresponding 0.166, 0.08, and 0.04 g of TOAB in 40 mL of THF was taken and to that a constant quantity (6.30 mL) of 9.65×10^{-3} M H_2PtCl_6 in THF was added. The solution was stirred under the flow of N_2 gas for 16 h at room temperature. The initial color of the solution was yellow. After 16 h stirring, the color of the solution became deep orange yellow. To this solution, 40 mL of 98% of HCOOH acid was added and the mixture was refluxed at 90 °C for 5 h. The resulting mixture was a light greenish brown color, indicating the formation of Pt colloids. Then, the excess reducing agent and solvent present in the mixture were evaporated at 60 °C. After removing all the organic substances, a brown waxy residue of Pt colloids was formed and subsequently it was dried in a vacuum oven overnight at room temperature. To this residue, methanol and DI water (6:4 ratio) were added with stirring. A clear brown color solution was formed, and then it was ultrasonicated for 5−10 min. A control catalyst without the presence of TOAB was also synthesized by using a similar procedure for comparison purposes.

Loading of Pt Colloids on Vulcan XC-72. The Vulcan XC-72 carbon was taken in water and methanol mixture (6:4 ratio) and ultrasonicated for 30 min to produce a well dispersed carbon ink. The synthesized Pt colloidal solution was then, added drop by drop to the carbon ink with constant stirring. The resulting heterogeneous catalyst mixture was allowed to stir for overnight and then filtered and dried in a vacuum oven for 2 h at 70 °C. The filtrate was found to be colorless and analyzed for the presence of Pt metal if any. The results of ICPAES showed the absence of Pt metal in the filtrate, which indicated the complete adsorption of Pt particles onto the surface of the carbon.

Removal of Surfactant from Catalyst. To remove the surfactant TOAB from the Pt/C nanocatalysts, three different approaches were followed:

(i) The catalytic powders were dispersed in ethanol and ultrsonicated for 15 min. Then, they were centrifuged in excess ethanol at the speed of 17 000 rpm for 10 min and the treated ethanol was siphoned off. This centrifugation process was repeated six times. Finally, the catalysts were dried in a vacuum oven at 70 °C for 2 h to remove the trace amount of alcohol.

(ii) The catalysts were subjected to annealing at 500 °C in a flow of N_2 gas (250 mL/min) for 4 h, following the ethanol treatment as mentioned above.

(iii) The catalysts were subjected to annealing treatment alone at 500 °C in a flow of N_2 gas (250 mL/min) for 4 h.

From the XPS and CV studies, it is understood that the ethanol treatment alone can be sufficient to get rid of the TOAB from the catalytic particles. Hence the forthcoming catalytic investigations will be referred to only to the ethanol-treated catalysts unless otherwise mentioned.

Preparation of Working Electrode. Glassy carbon (GC) (Taizhou electroanalytical instrument factory, China, 4 mm diam, 0.125 cm^2) was polished to a mirror finish with 0.05 μm alumina suspension before each experiment and served as an underlying substrate of the working electrode. The catalyst ink was prepared by ultrasonically dispersing 7.2 mg of 20 wt % of Pt/C in 2.5 mL of ethanol, to which 0.5 mL of 0.1 wt % of Nafion solution was added and the dispersion was then ultrsonicated for 30 min. A quantity of 10 μL of the dispersion was pipetted out on the top of the GC and over which 10 μL of 0.1 wt % of Nafion was added. Then, the electrode was dried at 80 °C to yield a Pt loading of 48 $\mu g/cm^2$.

Electrocatalytic Measurements. Electrocatalytic measurement was carried out using Autolab potentiostat (Eco chemie Co., Netherlands). A conventional, three-electrode cell consisting of the GC (0.125 cm^2) working electrode, Pt wire, as counter electrode, and Ag/AgCl reference electrode was used for the cyclic voltammetry (CV) experiment. The reference electrode was placed in a separate chamber, which is located near the working electrode through a Luggin capillary tube. The CV experiments were performed in 0.5 M H_2SO_4 solution in the absence and presence of 1 M CH_3OH at a scan rate of 50 mV/s. All the solutions were prepared by using ultrapure water (Millipore, 18 MΩ). N_2 gas was purged for nearly 30 min before starting the experiment, and stable voltammograms recorded after 10 cycles were taken into account for all the CV experiments.

Results and Discussion

Electron Microscopy Study. Size distributions of the Pt particles loaded on carbon are evaluated by TEM analysis. Figure 1 presents the TEM images of 20 wt % of Pt/C synthesized at N/Pt molar ratios of 0.76, 0.38, and 0.19 and the control catalyst. In the 0.76 ratio catalyst, as noted in Figure 1a, the dark spots of Pt nanoparticles have a uniform and extremely narrow size distribution with an average diameter of 2.2 nm. For the 0.38 ratio catalyst, the image shows a slight increase in the size of the Pt particles (2.5−3 nm). Besides, a nonuniform distribution of the particles is observed in some parts of the carbon (see Figure 1b). The very low (0.19) molar ratio catalys not only has an increment in the size of particles (3−4 nm), but also has very poor distribution of the particles as seen in Figure 1c. Contrarily, in the control catalyst, as expected, some big particles are observed with severe aggregation and it is very difficult to exactly measure the particle size under these conditions, but a rough estimation gives the particle size of 30 nm (see Figure 1d). It is obvious from these results that the size of the Pt particles increases with decreasing molar ratio, and eventually the particles grow uncontrollably with severe aggregation in the absence of surfactant. A similar dependence of particle size on the molar ratio between the surfactant and the precursor was observed in the synthesis of homogeneous Pt nanoparticles by reduction of chloroplatinic acid with sodium borohydride.[16]

The TEM image of the N/Pt ratio of 0.76 catalyst, which is annealed at 500 °C in a flow of N_2 gas for 4 h followed by the ethanol treatment, is shown in Figure 1e. It can be seen from the picture that the size of the Pt particles is increased (3−4 nm) compared with that of the unheated catalyst. Hence it is clear that the further annealing treatment leads to some undesirable agglomeration of the particles.

Figure 2 is the histogram of the size distribution measured from the well-separated particles obtained from the enlarged TEM picture of the 0.76 ratio catalyst both in unheated and heated conditions (Figure 1a,d). The mean sizes of Pt nanoparticles are 2.2 and 3.6 nm, respectively, for the former and later conditions, with a standard deviation of 0.5 nm.

XRD Analysis. Figure 3 displays the XRD patterns of the three different molar ratios (0.76, 0.38, and 0.19) of 20 wt % of Pt/C. All the molar ratio catalysts exhibit the characteristic diffraction peaks of Pt (111) at 2θ of 39.79°, Pt (200) at 2θ of 46.3°, and Pt (220) at 2θ of 67.45°, indicating the successful reduction of metal salt to Pt, which is present in the face centered cubic (fcc) phase. For comparison, the result for E-TEK 20% Pt/C is also presented. The peaks that appear at 2θ of 25° are associated with the presence of Vulcan XC-72 carbon as the supporting material. From the line broadening of (111) peak at 2θ of 39.79° by using the Scherrer equation after background subtraction, the average sizes of the particles of the catalysts, viz., ratios of 0.76, 0.38, 0.19, and E-TEK are estimated to be 2.1, 2.4, 4.1 nm, and 2.8 nm, respectively. These data are in good agreement with those of the TEM results. From the TEM and XRD analyses, it is evident that the Pt/C nanocatalyst synthesized with the N/Pt molar ratio of 0.76 has smaller platinum particles (2.2 nm) with uniform and well-defined dispersions. Hence, further discussions will be mainly focused on the nanocatalysts synthesized at this condition.

Surface Characterization of Nanocatalyst by XPS. Figure 4 shows the narrow scan of Pt (4f) core level of XPS of 20 wt % of Pt nanocatalyst synthesized with a N/Pt ratio of 0.76. The spectrum shows a doublet containing a low energy band ($4f_{7/2}$) at 71.3 eV, and a high energy band ($4f_{5/2}$) centered at 74.6 eV, which is 3.33 eV higher than the low energy band. The lower energy band at 71.3 eV agrees well with the published data of Pt metal at 71.1 eV.[17] The area ratio between $4f_{7/2}$ and $4f_{5/2}$ components is 4/3, which is consistent with the literature values.[18] On seeing the nature of two components present in the XPS spectrum, there can be a possibility for the presence of two different Pt entities on the surface. To identify the different entities, the spectrum could be curve-fitted to two pairs of Pt (4f) peaks at 71.3 and 74.7, and at 72.6 and 76.13 eV, respectively, as shown in Figure 4. These two pairs of peaks indicate the existence of two different Pt oxidation states, namely Pt(0) and Pt (II), and the percentages of these two species are calculated from the relative intensities of these peaks and are given as 73.64 and 26.36%, respectively. The percentage of Pt-(0) species (73.64%) present in the nanocatalyst synthesized by our method is equivalent to that of the E-TEK catalyst and higher than those values reported in the literature (see Table 1).[10,19] The existence of the Pt(II) state, i.e., PtO species, is quite common because some fine metallic Pt particles are always covered with chemisorbed oxygen as reported in the literature.[19,20] In addition, the surface atomic composition determined by the spectrum shows the Pt loading level of 23% which is slightly higher than the real weight percentage (20 wt %) taken to prepare the catalyst. As XPS could analyze more than just the top surface layer (5−8 nm in depth), it is difficult to know the real atomic composition. From the XPS results, it is inferred

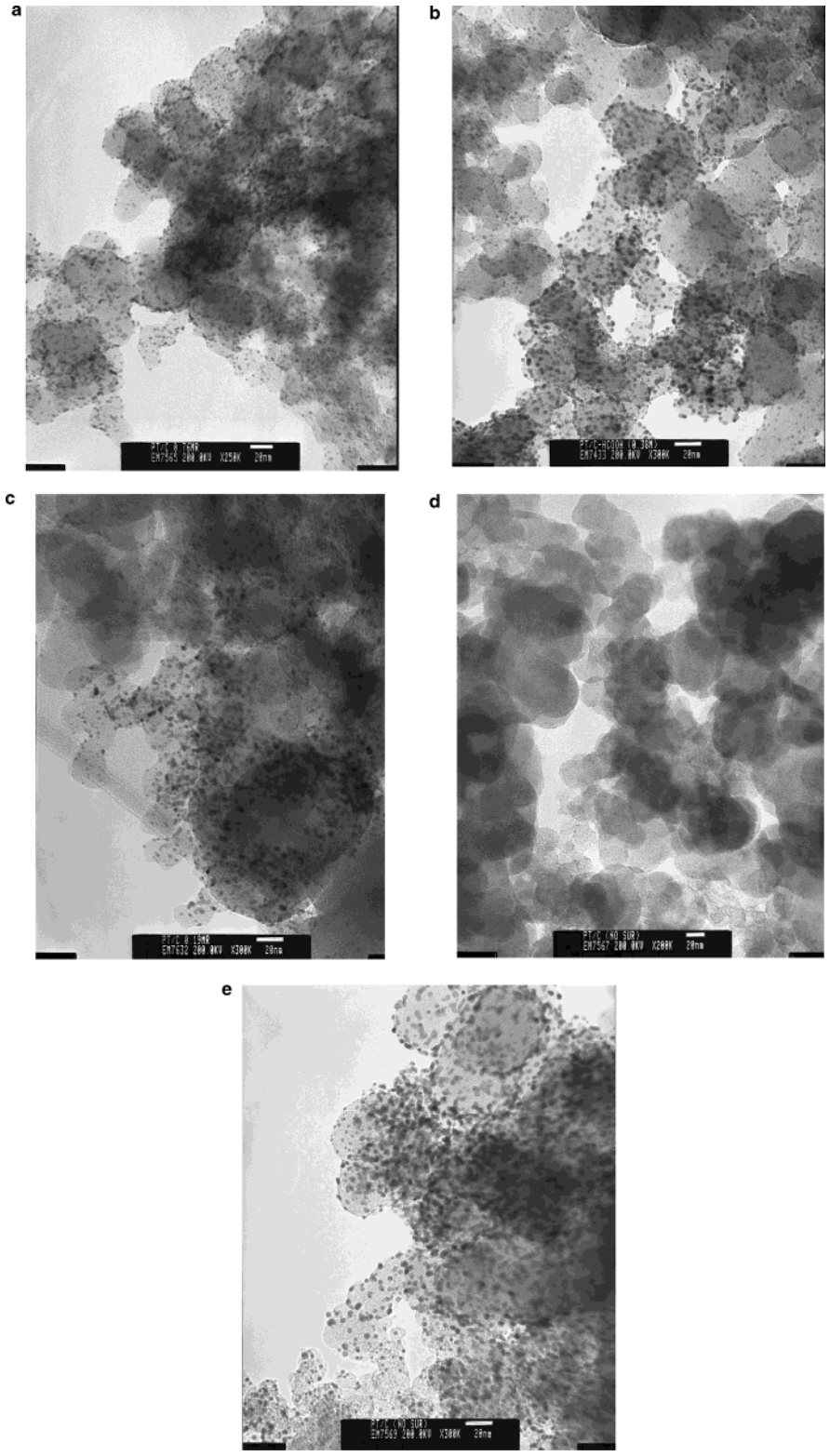

Figure 1. Transmission electron micrographs of 20 wt % Pt/C synthesized at different conditions: (a) N/Pt ratio of 0.76, (b) N/Pt ratio of 0.38, (c) N/Pt ratio of 0.19, (d) control catalyst, and (e) N/Pt ratio of 0.76 (annealed at 500 °C in N_2 atm).

that the enrichment of Pt(0) species can be accomplished in the Pt/C nanocatalyst synthesized with N/Pt ratio 0.76.

Stabilization Effect of TOAB. Stabilization of the Pt particles by TOAB can be discussed mainly from the viewpoint of electrostatic effect because of the cationic nature of the surfactant TOAB. The tetraalkylammonium ions (NR_4^+) surrounding the negatively charged metal core of the particles inhibit the particles from undergoing any kind of agglomeration. The coverage of the metal particles by the large lipophilic alkyl groups exerts a remarkable stability to the particles. It is worthwhile to mention the study of Bonnemann et al.[1a] who made an extensive investigation on the stabilization mechanism in their synthesis of homogeneous catalyst using the surfactant TOAB combined with the reducing agent $K[BEt_3H]$ in THF. They explained that the NR_4^+ ions, which are formed in a high local concentration at the reduction center, act as an efficient protecting agent against any agglomeration of the metal particles. In the present investigation, a different preparative approach

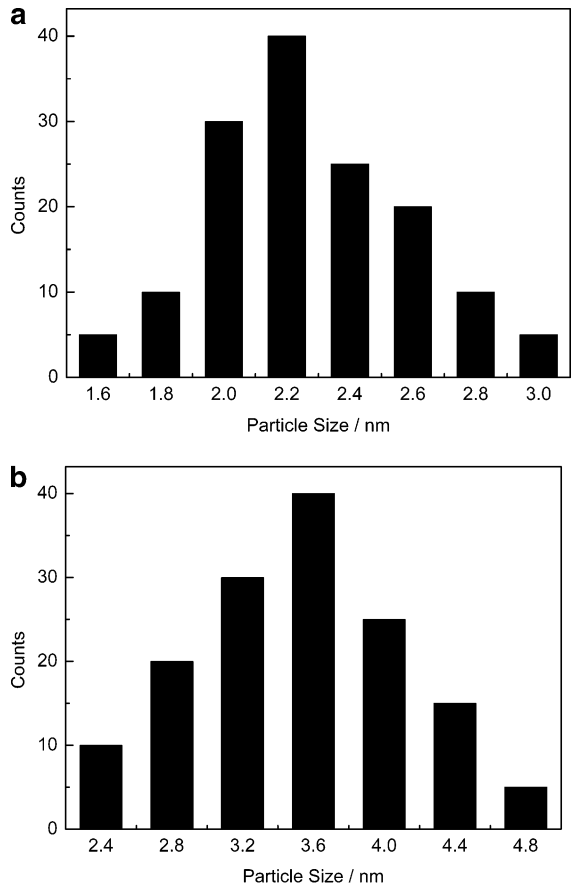

Figure 2. Histogram of Pt particle size distribution on carbon for the N/Pt ratio of 0.76: (a) without annealing, and (b) with annealing at 500 °C in N_2 atm.

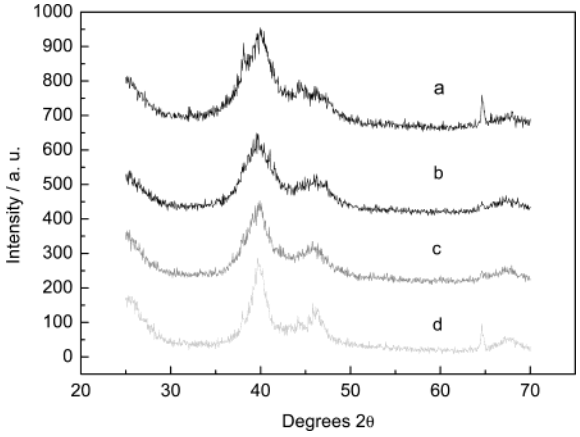

Figure 3. XRD patterns of 20 wt % of Pt/C: (a) E-TEK, (b) N/Pt ratio of 0.76, (c) N/Pt ratio of 0.38, and (d) N/Pt ratio of 0.19.

has been adopted, where the stabilizing agent is coupled with the metal salt prior to the reduction step. However, it is still believed that a similar stabilization effect may hold good to prevent the particles from any kind of agglomeration. Of the three N/Pt ratios (0.76, 0.38, and 0.19), the stabilization effect is more pronounced in the 0.76 ratio, which in turn leads to the formation of smaller particles with uniform dispersion over the carbon support as evident from the TEM image (see Figure 1a). This is probably because of a higher molar ratio of TOAB/Pt, a strong coordination affinity of the surfactant with $PtCl_6^{2-}$ ions could be realized, and thereby causing a decrease in the rate of reduction of $PtCl_6^{2-}$ ions. On the other hand, this strong hydrophobic interaction of TOAB with the Pt particles prevents

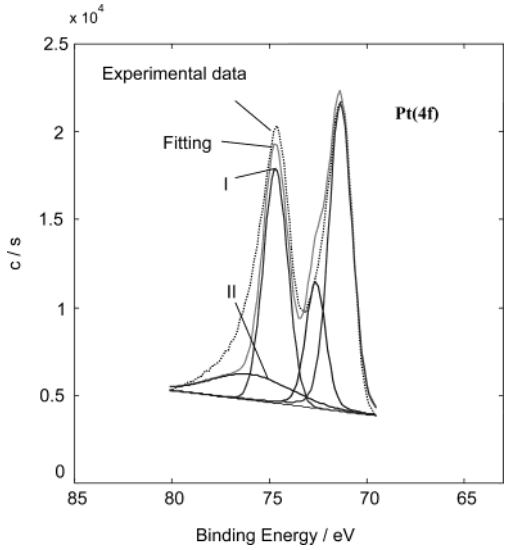

Figure 4. XPS of Pt (4f) of 20 wt % Pt/C obtained at N/Pt ratio of 0.76.

TABLE 1: Binding Energies and Relative Intensities of Different Platinum Species As Observed from Pt (4f) XPS of 0.76 Ratio Pt/C, E-TEK, and Pt/C Catalysts Synthesized by Other Methods

catalyst and preparative methods	species	binding energy of $4f_{7/2}$/eV	relative intensity %
Pt/C catalyst synthesized in this study	Pt(0)	71.3	73.64
	Pt(II)	72.6	26.36
E-TEK catalyst	Pt(0)	71.2	73.54
	Pt (II)	72.4	26.46
Pt/C catalyst[a]	Pt (0)	70.6	70.6
	Pt(II)	72.8	19.0
	Pt (IV)	74.2	8.0
Pt/nanotube catalyst[b]	Pt (0)	71.0	67.3
	Pt (II)	72.2	32.7

[a] Reference 19. [b] Reference 10.

or slows down the migration and agglomeration of the metal particles. Thus, the lower rate of reduction and the consequent inhibition in the agglomeration of particles led to the formation of smaller particle sizes in a higher molar ratio (0.76) catalyst relative to that of the lower molar ratios (0.38 and 0.19). This type of complex formation between the surfactant and the metal ions, which controls the free metal ions and the resultant reduction into smaller particles have been reported by Yonezawa et al.[21] and Torigoe et al.[22] in their preparation of Pt and Au nanoparticles, respectively. Therefore, it is proposed that the increase in size of the particles on decreasing the N/Pt ratio (decreasing the concentration of TOAB) may be due to the incomplete coverage of TOAB molecule on the particle surface.

XPS Investigations To Prove the Coverage of Pt Particles by a Stabilizing Agent. The coverage of the Pt particles by the TOAB has been investigated by the XPS spectra and is shown in Figures 5 and 6. The survey scan of the XPS for the freshly synthesized 20 wt % Pt/C nanocatalyst (N/Pt ratio of 0.76) which has not been subjected to ethanol and annealing treatment is shown in Figure 5. It is evident from the spectra that apart from the very strong signals due to C(1s), Pt(4f), and O (1s), a strong signal of N(1S) is also seen. To study the nature of the N in detail, the regional N (1S) XPS spectra is recorded and shown in Figure 6. A prominent N (1S) signal appears at 402.7 eV. Even for other lower N/Pt molar ratio catalysts (0.38 and 0.19), this signal appears in the same binding energy

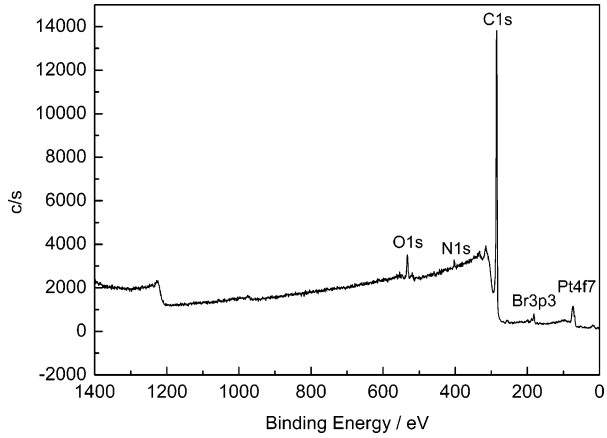

Figure 5. The survey scan of XPS of 20 wt % Pt/C obtained at N/Pt ratio of 0.76.

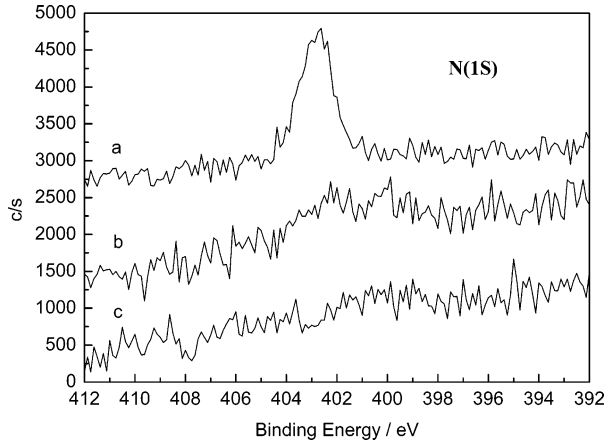

Figure 6. XPS of N (1S) for 20 wt % Pt/C at N/Pt ratio of 0.76: (a) before ethanol and annealing treatment, (b) after treatment with ethanol, and (c) annealed at 500 °C in N_2 atm for 4 h, after the ethanol treatment.

position (402.7 eV), but with less intensity (figures not shown). This can be attributed to the adsorption of the stabilizing agent quarternary ammonium ions (NR_4^+) over the surface of the Pt particles through head-on N atom. Schmidt et al.[15a] also observed a similar type of N(1S) signal at 402.3 eV, in their XPS investigation for the Pt−Ru colloid stabilized by TOAB. These results have provided sufficient evidence for the presence of N atoms that could have hydrophobic interaction and coordination affinity with the particles of Pt and protect them from the agglomeration process that is commonly encountered in the absence of stabilizing agents.[23]

Removal of TOAB Followed by XPS. The removal of the stabilizing agent TOAB by way of treatment with ethanol and subsequent annealing at high temperature, which is necessary for the electrochemical measurements, is followed by XPS. After centrifugation of the catalyst in excess ethanol for six times, the N(1S) peak almost disappears and further annealing at 500 °C in a flow of N_2 gas for 4 h, the N(1S) peak can no longer be detected (see Figure 6). This implies that the complete removal of the stabilizing agent from the surface of the Pt particles could be achieved by the ethanol treatment alone. Though the annealing step has further helped to completely get rid of the stabilizing agent, this leads to an undesirable agglomeration of the Pt particles, as seen in the TEM image of Figure 1e. The complete removal of the stabilizing agent (after the ethanol treatment) has helped to increase the intensity of the Pt (4f) peak that has been discussed in Figure 4. To remove similar stabilizing agent from the Pt−Ru/C catalyst, Schmidt et al.[15a] followed the annealing steps, where the sample was first heated in oxygen and then in hydrogen at 300 °C for 30 min. They could remove the surfactants completely from the catalyst; however, the size of the particles had grown to some extent as we have noted in our results. Hence, it is advocated that the surfactant TOAB could be easily eliminated from the catalyst simply by treating with ethanol, and no longer imposes a poisoning effect to the catalyst. This claim will further be proved in the electrochemical studies in the following section. Boutonett et al.[24] suggested the view that the surfactant has no poisoning effect in the catalytic reaction and it could be eliminated by washing with alcohol, followed by heat treatment of the catalyst.

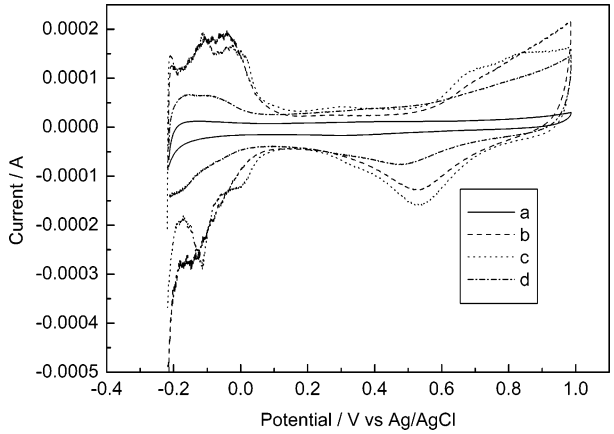

Figure 7. CV of 20 wt % of Pt/C synthesized at N/Pt ratio of 0.76 in 0.5 M H_2SO_4 followed by various treatments: (a) before treatment with ethanol, (b) after treatment with ethanol, (c) annealed at 500 °C in N_2 atm for 4 h, after the ethanol treatment, and (d) annealed at 500 °C in N_2 atm for 4 h.

Electrochemical Behavior of Treated and Untreated Catalysts. Figure 7 shows the voltammograms of the treated and untreated 20 wt % Pt/C (0.76 ratio) in 0.5 M H_2SO_4 solution. The catalyst that is synthesized as such (prior to the ethanol and heat treatment) shows no characteristic features in the hydrogen and oxygen adsorption−desorption regions, suggesting that the covered surfactant molecules completely block the active sites of the Pt particles. For the catalyst that is subjected to annealing at 500 °C in N_2 atm, less pronounced hydrogen adsorption−desorption features with very small current values appeared both in the anodic and cathodic sweeps. The obtained voltammetric profile indicates a partially blocked surface, perhaps due to the decomposition of carbonaceous species or coke generated from TOAB decomposition in nitrogen atmosphere. On the other hand, for the ethanol treated catalyst, well-defined profiles are observed in the hydrogen adsorption−desorption regions, which in turn prove the high surface area of the catalyst. This has indicated that the TOAB molecules are completely eliminated from the surface of the Pt particles. The voltammetric features of the catalyst that is annealed at 500 °C in N_2 atm after the ethanol treatment appears to be similar to that of the ethanol-treated catalyst. Additionally, it exhibits three anodic and two cathodic sharp peaks in the hydrogen adsorption−desorption region, respectively. The formation of these sharp peaks can be attributed to the increase in the size of the Pt particles after the annealing treatment as shown in the TEM picture (see Figure 1e). This result is in good agreement with the finding of Kinoshita,[25] who suggested that the specific activity (activity based on the surface area) increases with the diameter of the particles. The voltammetric results have further substantiated our argument that the ethanol

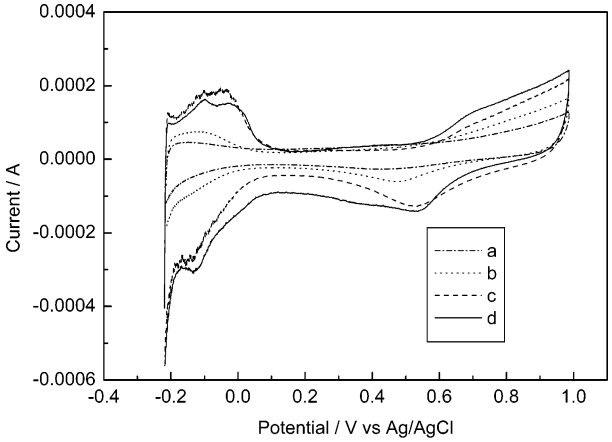

Figure 8. CV of 20 wt % of Pt/C synthesized at different N/Pt ratios: (a) 0.19, (b) 0.38, (c) 0.76, and (d) E-TEK catalyst in 0.5 M H_2SO_4 solution.

TABLE 2: Electrochemical Surface Areas of Pt/C Electrocatalysts at Different N/Pt Ratios[a]

Pt/C electrocatalysts	electrochemical surface area (cm^2)
E-TEK catalyst	2.87
catalyst at N/Pt ratio of 0.19	1.75
catalyst at N/Pt ratio of 0.38	2.06
catalyst at N/Pt ratio of 0.76	3.24

[a] All the calculations are based on a proportionality constant of 210 $\mu C/cm^2$ for platinum metal.

treatment alone is the efficient way of removing the surfactant TOAB from the catalytic particles.

Electrochemical Behavior of Three N/Pt Molar Ratio Catalysts. The voltammograms of the 20 wt % Pt/C synthesized with N/Pt molar ratios of 0.76, 0.38, and 0.19 and E-TEK catalyst in 0.5 M H_2SO_4 solution are shown in Figure 8. For the 0.19 ratio catalyst, a very poorly resolved peak is observed in the hydrogen adsorption−desorption region. The 0.38 ratio catalyst exhibits a broad peak relatively with slightly higher current in the adsorption−desorption region than the 0.19 ratio catalyst. This is probably due to agglomeration and poor dispersion of the Pt particles in these lower molar ratio catalysts. These problems are highly pronounced, especially in 0.19 ratio catalyst, as evident from the TEM picture (see Figure 1c). Conversely, for the 0.76 ratio catalyst, well-defined hydrogen adsorption−desorption peaks with a much larger area are observed in the potential region −0.22 to 0.04 V, demonstrating the higher surface area of the catalyst. The high surface area is owing to the presence of narrow size and uniform distribution of the Pt particles as displayed in the TEM picture (see Figure 1a). Electrochemical surface areas of Pt/C electrocatalysts at different N/Pt ratios are listed in Table 2. These values are obtained by calculating the areas under the hydrogen desorption peaks (see Figure 8) after subtracting the contribution from double layer charging. It was found that, when the N/Pt ratio is higher than 0.76, its effect on the particle size is negligible. Most of the Pt colloids can be stabilized in the solution at a N/Pt ratio of 0.76 or higher. By controlling the amount of carbon black added to the Pt colloids, catalysts with different Pt loadings can be prepared.

The features in the hydrogen adsorption−desorption region can normally be rationalized on the basis of hydrogen electrochemistry on low-index single-crystal platinum electrodes in acid solutions.[26,27] The broad and featureless H-desorption peak observed for the 0.76 ratio catalyst in the potential region −0.22 to 0.04 V indicates the presence of Pt(111) sites. This observation is consistent with the literature data and explains the fact that the nanostructure of platinum is composed of low-coordination-number single crystals.[28]

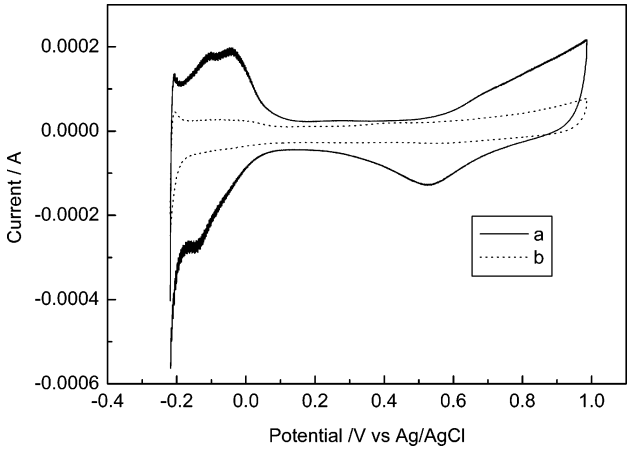

Figure 9. CV of 20 wt % Pt/C: (a) catalyst at N/Pt ratio of 0.76, and (b) control catalyst in 0.5 M H_2SO_4 solution.

While considering the oxide reduction peak potentials, the peak potential of the 0.76 ratio catalyst is shifted to the negative side compared to that of the 0.38 ratio catalyst. This may be due to the influence of different sizes of particles on oxide reduction potentials as reported by some researchers.[29,30] These results have confirmed that the 0.76 ratio catalyst has a higher electrochemical surface area relative to that of the lower molar ratio catalysts.

In Figure 9, the voltammetric feature of the 0.76 ratio catalyst is compared with the control catalyst in 0.5 M H_2SO_4 solution. The control catalyst has not shown any well-defined profiles in the hydrogen adsorption regions such as appeared in the 0.76 ratio catalyst. This may be owing to the problem of severe aggregation of the particles that occurred in the absence of surfactant TOAB as shown in the TEM image (Figure 1d). Furthermore, the absence of any well-defined profiles in the hydrogen adsorption regions as that appeared in the 0.76 ratio catalyst may be due to the limited amounts of Pt (111) and Pt (100) faces.

Evalution of Methanol Electro-oxidation Activity of Pt/C Nanocatalysts. The cyclic voltammograms of all the three molar ratios and E-TEK catalysts in 0.5 M H_2SO_4 + 1 M CH_3OH solution are presented in Figure 10. Among the three different molar ratio catalysts, the 0.76 ratio catalyst exhibits a higher methanol oxidation current. For this catalyst, the onset potential of methanol oxidation occurs at 0.22 V, which is relatively more negative than that of the other catalysts. This may be attributed to the easier formation of Pt−OH species on the smaller 0.76 ratio catalyst. These Pt−OH species can facilitate oxidation of methanol adsorbates on the adjacent sites. This assumption is in good agreement with the study of Frelink et al.,[30] who made an elaborate investigation on the particle size effect on methanol oxidation and concluded that small sized particles favor oxide formation in the lower potential region.

Although the surface areas (see Table 2) for both the 0.76 ratio catalyst and E-TEK catalyst are comparable, the methanol oxidation current of the former is much higher than that of the later. The observation of this phenomenon is not well understood here, and further investigation would be required in this line. The small difference noted in the position of peak potentials both for the forward and backward scan may be related to the position of oxide reduction potentials. Frelink et al.[30] also

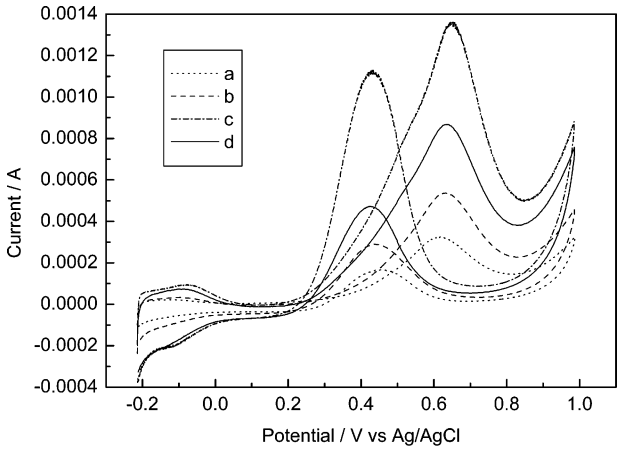

Figure 10. CV of 20 wt % of Pt/C synthesized at different N/Pt ratios: (a) 0.19, (b) 0.38, (c) 0.76, and (d) E-TEK catalyst in 0.5 M H_2SO_4 + 1 M CH_3OH solution.

observed a similar type of peak position changes in the course of their investigation of methanol oxidation on nanocatalysts of different sizes.

Conclusions

The platinum nanocatalysts supported on Vulcan XC-72 carbon are synthesized with different molar ratios of TOAB to chloroplatinic acid (N/Pt ratio of 0.76, 0.38, and 0.19) using formic acid as the reducing agent in the solvent THF. A control catalyst without the presence of TOAB is also synthesized and compared. The morphological properties of these catalysts are evaluated by the TEM and it is found that the 0.76 ratio catalyst has well-separated smaller particles (2.2 nm) than those of the lower molar ratio and control catalysts. The XRD analysis indicates the formation of Pt in the fcc phase, and the average size of the particles calculated from XRD peak widths are consistent with the TEM results. From these results, it is concluded that the size of the particles increases with the decrease of the N/Pt ratio. The XPS measurements reveal that the 0.76 ratio catalyst has higher amount of platinum present in its metallic state (73. 64% of Pt(O) and 26.36% of Pt(II)), which is equivalent to that of the E-TEK catalyst. The stabilization process of the TOAB on the surface of the platinum particles appears to be effective for the catalyst with N/Pt ratio of 0.76. The XPS investigations have proved the presence of coverage of the TOAB and its subsequent removal from the surface of the Pt particles, which is the necessary step prior to the electrochemical measurements. The removal of the TOAB is carried out by annealing the catalyst at 500 °C in a flow of N_2 gas for 4 h, followed by the treatment with ethanol. It is found that the ethanol treatment is an efficient way to get rid of the TOAB without imposing any undesirable changes to the catalytic particles. Finally, the cyclic voltammetric response reveals that the surface area and the methanol oxidation current of the 0.76 ratio catalyst is higher than that of the lower molar ratios (0.38 and 0.19) and control catalysts and is equivalent or slightly higher than that of the E-TEK catalyst.

Acknowledgment. The authors gratefully acknowledge the Innovation and Technology Commission of Hong Kong SAR Government (ITS/176/01A) for the funding support.

References and Notes

(1) (a) Bonnmann, H.; Brijoux, W.; Brinkmann, R.; Dinjus, E.; Fretzen, R.; Joussen, T.; Koppler, B.; Korall, B.; Neiteler, P.; Richter, J. *J. Mol. Catal.* **1994**, *86*, 129. (b) Bonnemann, H.; Braun, G.; Brijoux, W.; Brinkmann, R.; Tilling, S.; Seevogel, K.; Siepen, K. *J. Organomet. Chem.* **1996**, *520*, 143. (c) Bonnemann, H.; Britz, P. *Langmuir* **1998**, *14*, 6654. (e) Wang, X.; Hsing, I.-M. *Electrochim. Acta* **2002**, *47*, 2981. (f) Umeda, M.; Kokubo, M.; Mohamedi, M.; Uchida, I. *Electrochim. Acta* **2003**, *48*, 1367. (g) Park, S.; Xie, Y.; Weaver, M. J. *Langmuir* **2002**, *18*, 5792. (h) Lee, A. S.; Park, K. Y.; Choi, J. H.; Kwon, B. K.; Sung, E. Y. *J. Electrochem. Soc.* **2002**, *149* (10), A1299. (i) Gullon, S. J.; Montiel, V.; Aldaz, A.; Clavilier, J. *J. Electrochem. Soc.* **2003**, *150* (2), E104. (j) Steigerwalt, E. S.; Deluga, A. G.; Lukehart, C. M. *J. Phys. Chem. B* **2002**, *106*, 760.

(2) Ross, P. N. *Electrocatalysis*; Lipkowski, J., Ross, P. N., Eds.; Wiley-VCH: New York, 1998; Chapter 2.

(3) Mukerjee, S.; McBreen, J. *J. Electroanal. Chem.* **1998**, *448*, 163.

(4) Tong, Y. Y.; Rice, C.; Wieckowski, A.; Oldfield, E. *J. Am. Chem. Soc.* **2000**, *122*, 1123.

(5) Park, S.; Wasileski, A.; Weaver, M. J. *J. Phys. Chem. B* **2001**, *105*, 9719.

(6) Kinoshita, K. *Modern Aspects of Electrochemistry*; Bockris, J. O′ M., Conway, B. E., White, R. E., Eds.; Plenum Press: New York, 1982; Vol. 14, p 557.

(7) Mukerjee, S. *J. Appl. Electrochem.* **1990**, *20*, 537.

(8) (a) Che, G.; Lakshmi, B. B.; Fisher, R. E.; Martin, R. E. *Nature* **1998**, *393*, 346. (b) Che, G.; Lakshmi, B. B.; Fisher, R. E.; Martin, R. E.; Fisher, R. E. *Langmuir* **1999**, *15*, 750.

(9) (a) Rajesh, B.; Karthik, V.; Karthikeyan, S.; Ravindranathan Thambi, T.; Bonard, J.-M.; Viswanathan, B. *Fuel* **2002**, *81*, 2177. (b) Rajesh, B.; Ravindranathan Thambi, T.; Bonard, J.-M.; Xanthopoulos, N.; Mathieu, J. H.; Viswanathan, B. *J. Phys. Chem. B* **2003**, *107*, 2701.

(10) Liu, Z.; Lin, X.; Lee, J. Y.; Zhang, W.; Han, M.; Gan, L. M. *Langmuir* **2002**, *18*, 4054.

(11) Xue, B.; Chen, P.; Hong, Q.; Lin, J.; Tan, L. K. *J. Mater. Chem.* **2001**, *11*, 2378.

(12) Hermans, S.; Sloan, J.; Shephard, S. D.; Johnoson, B. F. G.; Malcolm, L. H. *Chem. Commun.* **2002**, 276.

(13) Serp, P.; Feurer, R.; Kihn, Y.; Kalck, P.; Faria, L. J.; Figueiredo, L. J. *J. Mater. Chem.* **2001**, *11*, 1980.

(14) (a) Steigerwalt, S. E.; Deluga, A. G.; Cliffel, E. D.; Lukehart, M. C. *J. Phys. Chem. B* **2001**, *105*, 8097. (b) Steigerwalt, S. E.; Deluga, E. D.; Lukehart, M. C. *J. Phys. Chem. B* **2002**, *106*, 760.

(15) (a) Schmidt, T. J.; Noeske, M.; Gasteiger, A. H.; Behm, R. J.; Britz, P.; Brijoux, W.; Bonnemann, H. *Langmuir* **1997**, *13*, 2591. (b) Schmidt, T. J.; Noeske, M.; Gasteiger, A. H.; Behm, R. J.; Britz, P.; Brijoux, W.; Bonnemann, H. *J. Electrochem. Soc.* **1998**, *145* (3), 1998. (C) Paulus, U. A.; Endruschat, U.; Feldmeyer, G. J.; Schmidt, T. J.; Bonnemann, H.; Behm, R. J. *J. Catal.* **2000**, *195*, 383.

(16) Chen, S.; Kimura, K. *J. Phys. Chem. B* **2001**, *105*, 5397.

(17) Hufner, S.; Wertheim, G. K. *Phys. Rev. B* **1975**, *11*, 678.

(18) Moulder, J. F.; Stickle, W. F.; Sobol, P. E.; Bomben, K. D. *Handbook of X-ray Photoelectron Spectroscopy*; Chastain, J.; Ed.; Perkin-Elmer Corp.: Eden Praire, MN, 1992; p 181.

(19) Shukla, A. K.; Neergat, M.; Bera, P.; Jayaram, V.; Hegde, S. M. *J. Electroanal. Chem.* **2001**, *504*, 111.

(20) Arico, A. S.; Creti, P.; Modica, E.; Monforte, G.; Baglio, V.; Antonucci, V. *Electrochim. Acta* **2000**, *45*, 4319.

(21) Yonezawa, T.; Tominaga, T.; Toshima, N. *Polym. Adv. Techn.* **1996**, *7*, 645.

(22) Torigoe, K.; Esumi, K. *Langmuir* **1992**, *8*, 59.

(23) Chow, G. M.; Gonsalves, K. E. In *Nanomaterials: Synthesis, properties and applications*; Edelstein, A. S., Cammarata, R. C., Eds.; American Institute of Physics: Woodbury, NY, 1996; p 55.

(24) Boutonnet, M.; Kizling, J.; Mintsa-Eya, V.; Choplin, A.; Touroude, R.; Maire, G.; Stenius, P. *J. Catal.* **1987**, *103*, 95.

(25) Kinoshita, K. *J. Electrochem. Soc.* **1990**, *137*, 845.

(26) Markovic, N. M.; Grgur, B. N.; Ross, P. N. *J. Phys. Chem. B* **1997**, *101*, 5405.

(27) Herrero, E.; Franaszczuk, K.; Wieckowski, A. *J. Phys. Chem. B* **1994**, *98*, 5074.

(28) Stonehart, P. *J. Appl. Electrochem.* **1992**, *22*, 995.

(29) Pauckert, M.; Yoneda, T.; Betta, R. A.; Boudart, M. *J. Electrochem. Soc.* **1986**, *133*, 944.

(30) Frelink, T.; Visscher, W.; Van Veen, J. A. R. *J. Electranal. Chem.* **1995**, *382*, 65.